

JAAS

Accepted Manuscript



This is an *Accepted Manuscript*, which has been through the Royal Society of Chemistry peer review process and has been accepted for publication.

Accepted Manuscripts are published online shortly after acceptance, before technical editing, formatting and proof reading. Using this free service, authors can make their results available to the community, in citable form, before we publish the edited article. We will replace this *Accepted Manuscript* with the edited and formatted *Advance Article* as soon as it is available.

You can find more information about *Accepted Manuscripts* in the [Information for Authors](#).

Please note that technical editing may introduce minor changes to the text and/or graphics, which may alter content. The journal's standard [Terms & Conditions](#) and the [Ethical guidelines](#) still apply. In no event shall the Royal Society of Chemistry be held responsible for any errors or omissions in this *Accepted Manuscript* or any consequences arising from the use of any information it contains.

1
2
3
4 1 **Single-step separation scheme and high-precision**
5
6 2 **isotopic ratios analysis of Sr-Nd-Hf in silicate**
7
8
9 3 **materials**
10
11
12 4

13
14 5 **Chao-Feng Li^{a*} Jing-Hui Guo^a Yue-Heng Yang^a**

15
16 6 **Zhu-Yin Chu^a Xuan-Ce Wang^b**
17
18
19 7

20
21 8 ^aState Key Laboratory of Lithospheric Evolution, Institute of Geology and
22
23 9 Geophysics, Chinese Academy of Sciences, Beijing 100029, China

24
25
26 10 ^bThe institute for Geoscience Research (TIGer), Curtin University, GPO Box U1987,
27
28 11 Perth, WA6845, Australia
29
30

31
32
33
34
35
36
37
38
39
40
41
42
43
44
45
46
47
48
49
50
51 20 *Corresponding author: Chao-Feng Li

52
53
54 21 E-mail address: cfli@mail.iggcas.ac.cn

55
56 22 Tel: +86-10-82998583
57
58
59
60

1
2
3
4
5
6
7
8
9
10
11
12
13
14
15
16
17
18
19
20
21
22
23
24
25
26
27
28
29
30
31
32
33
34
35
36
37
38
39
40
41
42
43
44
45
46
47
48
49
50
51
52
53
54
55
56
57
58
59
60

23 **Abstract:**

24 Thermal ionization mass spectrometry and multiple-collector inductively coupled
25 plasma mass spectrometry are considered “gold standards” for determining the
26 isotope ratios of Sr–Nd and Hf in geological samples because of the extremely high
27 precision and accuracy of these methods. However, the sample throughputs are
28 hindered by time-consuming and tedious chemical procedures. Three-step ion
29 exchange resin separation is traditionally employed to purify Sr-Nd-Hf from matrix
30 elements. In this study, a one-step Sr-Nd-Hf separation scheme is developed to
31 process geological samples. The separation scheme is based on the combined use of
32 conventional AG50W-X12 cation-exchange resin and LN Spec extraction
33 chromatographic material without any intervening evaporation step. The protocol not
34 only prevents cross-contamination during operation using multiple-stage ion exchange
35 resins but also significantly improves the efficiency of sample preparation. The
36 stability of our chemical procedure is demonstrated through replicate measurements
37 of $^{87}\text{Sr}/^{86}\text{Sr}$, $^{143}\text{Nd}/^{144}\text{Nd}$, and $^{176}\text{Hf}/^{177}\text{Hf}$ ratios in six international reference materials
38 of silicate rocks. The analytical results obtained for these standard rocks well agree
39 with the published data. The external reproducibility (2 SD, n = 10) of a BCR-2
40 standard sample was ± 0.000018 for $^{87}\text{Sr}/^{86}\text{Sr}$, ± 0.000010 for $^{143}\text{Nd}/^{144}\text{Nd}$, and \pm
41 0.000014 for $^{176}\text{Hf}/^{177}\text{Hf}$.

42
43
44 **Keywords:** Sr-Nd-Hf isotope ratios; Single-step separation; TIMS; MC-ICP-MS

1. Introduction

$^{87}\text{Sr}/^{86}\text{Sr}$, $^{143}\text{Nd}/^{144}\text{Nd}$ and $^{176}\text{Hf}/^{177}\text{Hf}$ ratios, which show variations by radioactive decay of long half life isotopes of ^{87}Rb , ^{147}Sm and ^{176}Lu , respectively, are routinely used for geochemistry as petro-genetic tracers, yielding information on time-integrated elemental fractionation through processes of melting, crystallization, metasomatism, and contamination.¹ In particular, the combination of radiogenic Sr-Nd-Hf isotope systems has become a more powerful tool for understanding fundamental Earth processes as well as the Earth's evolution. Thus, conducting multi-isotopic analyses (e.g., Sr-Nd-Hf) is critical on the same sample.

Thermal ionization source mass spectrometry (TIMS) and multiple-collector inductively coupled plasma mass spectrometry (MC-ICP-MS) both possess high accuracy, excellent sensitivity, and low memory. The methods are regarded as benchmark techniques for Sr-Nd and Hf isotopic ratio analysis and widely used in Earth science.²⁻¹² However, to obtain stable and high intensity of ion signals during TIMS and MC-ICP-MS measurements, Sr-Nd-Hf elements must be separated from sample matrices and be as clean as possible. Purification of Sr-Nd-Hf prior to mass spectrometric measurement is traditionally accomplished by using at least three-column chromatography after a single sample digestion.¹³⁻¹⁴ The first stage involves the separation of Hf from other elements using an anion resin¹⁵ or a special resin column, such as LN resin^{13, 16}, U-TEVA resin^{12, 14}, TEVA^{8, 17}, or TODGA resin.¹⁰ The discard from the first column is then dried and dissolved using HCl or HNO₃. Subsequently, Sr and rare earth elements (REEs) are separated from the matrix

1
2
3
4 67 elements using a second cation exchange resin column, such as a AG50W resin
5
6 68 column.^{2, 5-7, 11, 13, 14, 18, 19} Finally, Nd is separated from the REEs using a third resin
7
8 69 column, such as HDEHP resin column,^{2, 4-6, 11, 13, 14, 18-20} HEHEHP resin column⁷, A25
9
10 resin column and A27 resin column.²¹ Traditional three-step separation procedures
11
12 70 involve tedious pre-cleaning of the column and fraction evaporation. The traditional
13
14 71 multi-step chemical procedure takes at least three days to complete and large amounts
15
16 72 of reagents upon completion of column chemistry for a batch of geological samples
17
18 73 (e.g., 20~30 samples). Thus, the separation efficiency is low for traditional methods
19
20 74 and the sample throughput is impeded. In addition, traditional methods increase the
21
22 75 probability of contamination from cross-operation in column chemistry associated
23
24 76 with complex operation steps.
25
26
27
28
29
30

31 To the best of our knowledge, no available literature has reported the use of
32
33 79 analytical protocols to concomitantly separate Sr-Nd-Hf fractions from a single
34
35 80 sample digest using a one-step separation method. Yang²² and Li²³ recently presented
36
37 81 a method to precisely determine Nd isotopic ratios from the REEs using MC-ICP-MS
38
39 82 and TIMS. Based on this method, the traditional two-step Nd separation method was
40
41 83 simplified to a one-step procedure. More importantly, the method allowed Sr-Nd-Hf
42
43 84 isotopic determination using TIMS and MC-ICP-MS so long as high-purity Sr,
44
45 85 REE-enriched Nd, and Hf could be achieved. To this end, we present a one-column
46
47 86 separation procedure based on optimization of mixed cation resins (AG50W-X12 +
48
49 87 LN Spec).

50
51
52
53
54
55
56 88 The present study aims to reduce their rather extensive and costly cleaning and
57
58
59
60

1
2
3
4 89 separation procedures for resin and columns without negatively affecting the data
5
6 90 quality. This one-step separation route of obtaining Sr-Nd-Hf from a single
7
8
9 91 dissolution enables higher throughput for data acquisition by TIMS and MC-ICP-MS.
10
11 92 To verify the robustness of the new separation protocol for Sr-Nd-Hf, six certified
12
13 93 reference materials (CRMs) of silicate rocks, encompassing a wide range of matrix
14
15
16 94 compositions and analyte concentrations, were analyzed.
17
18
19 95

20 21 96 **2. Experimental**

22 23 97 **2.1 Reagents, chemicals materials and standards**

24
25
26 98 Re ribbon: 0.035mm thick, 0.77 mm wide and 99.98% pure, H.Cross Company.

27
28
29 99 Acids and water: All AR grade acids (hydrochloric acid, nitric acid and hydrofluoric
30
31 100 acid) were further purified using SavillexTM DST-1000 sub-boiling distillation system
32
33
34 101 (Minnetonka, USA). Phosphate acid was purified using chromatographic method of
35
36
37 102 AG50W-X12 resin manufactured by the Bio-Rad company. Ultrapure water with a
38
39 103 resistivity ($18.25 \text{ M}\Omega\cdot\text{cm}^{-1}$) was obtained from a Milli-Q Element system (Millipore,
40
41 104 USA) and used throughout this work for diluting concentrated acids.

42
43
44 105 Sr-Nd-Hf standard solutions: A stock solution of 100 ppm Sr and Nd was
45
46 106 gravimetrically prepared to monitor a Triton Plus TIMS instrument using NIST NBS-
47
48
49 107 987 and JNdi-1 reference materials. A JMC 475 Hf international standard solution of
50
51 108 100 ppb was used to monitor the stability of a Neptune Plus instrument.

52
53
54 109 Resin: Commercially available cation (AG50W-X12, 200-400 mesh size) and LN
55
56
57 110 Spec resin (100-150 μm) were obtained from Bio-Rad company and Eichrom

1
2
3
4 111 company.

5
6 112 Column: The cation-exchange polypropylene column was 7 cm long and had a 6 mm
7
8
9 113 i.d. and 5 mL reservoir. The column was packed with 1.5 mL of Bio-Rad
10
11 114 AG50W-X12 resin and 0.45 mL of LN Spe resin.

12
13
14 115 Rock standard samples: Rock powders of the CRMs were obtained from the United
15
16 116 States Geological Survey (USGS) and Geological Survey of Japan (GSJ). These
17
18 117 CRMS included USGS BCR-2 (basalt), BHVO-2 (basalt), W-2 (diabase),
19
20 118 BIR-1(basalt), GSJ JA-1(andesite), and JA-3 (andesite).

21
22
23 119 Labwares: The labware used included 15 and 7.0 mL PFA Teflon vials with screw top
24
25 120 lids (Savillex Corporation, USA). The vials were used for sample digestion, solution
26
27 121 collection, and evaporation and cleaned prior to use with a degreasing agent followed
28
29 122 by sequential washing in AR grade HNO₃, HCl, and ultra-pure H₂O.
30
31
32

33
34 123

35 36 124 **2.2 Sample digestion**

37
38
39 125 It was critical to achieve full recovery of Sr-Nd-Hf. Especially for Hf isotopic
40
41 126 ratio analysis, a critical point was the common occurrence of Zr + Hf-rich refractory
42
43 127 minerals, such as zircon, baddeleyite and garnet, which might host a major proportion
44
45 128 of the hafnium contained in the bulk rock. In previous studies, two digestion methods
46
47 129 were widely used in digestion geological samples: HF-HNO₃-HClO₄ mixture
48
49 130 dissolutions based on high-pressure PTFE bomb devices^{8, 11, 13, 15} and Lithium
50
51 131 metaborate or Na₂O₂ flux melting methods.^{10, 12, 24} The flux melting method had the
52
53
54 132 advantages of being rapid and ensuring full sample digestion regardless of mineralogy
55
56
57
58
59
60

1
2
3
4 133 or composition. However, the procedural blanks were high especially for Nd (~0.37
5
6 134 ng²⁴, ~1.5 ng⁹). The HF-HNO₃-HClO₄ mixture dissolutions based on high-pressure
7
8
9 135 PTFE bomb devices had the advantages of lower blanks. Furthermore, most isotope
10
11 136 laboratories had all the necessary equipments and experiences to immediately initiate
12
13 137 this method. It has the disadvantages of being slow (2~3 days). Considering the
14
15
16 138 potential blank effect from flux reagents, we adopt the dissolutions of
17
18
19 139 HF-HNO₃-HClO₄ mixture in this study.

20
21 140 All chemical preparations were conducted on special class 100 work benches
22
23 141 inside a class 1000 clean laboratory. Approximately 50~60 mg of rock powder
24
25 142 materials were weighed into a steel-jacketed acid-washed high-pressure PTFE bomb.
26
27 143 The samples were dissolved on a hotplate at 190 °C using an acid mixture of 3 mL of
28
29 144 29 M HF, 0.3 mL of 14 M HNO₃, and 0.3 mL of 11.8 M HClO₄ for 5 days. Usually, 2
30
31 145 ~3 days digestions were sufficient for most silicate samples. To obtain perfect sample
32
33 146 digestion, we prolonged the digestion time to 5 days in this study. All samples were
34
35 147 completely digested in this study. Digested samples were dried on a hotplate
36
37 148 overnight at ~ 120 °C and then reconstituted in 3 mL of 6 M HCl. This solution was
38
39 149 again dried at ~ 160 °C. Finally, the samples were re-dissolved with 1.1 mL of 2.5 M
40
41 150 HCl on a 100 °C hotplate overnight before commencing ion exchange chemistry.
42
43 151 Clear solutions of all sample fractions were obtained and no insoluble fluoride
44
45 152 compounds were found in this study.
46
47
48
49
50
51
52
53
54
55

56 154 **2.3 Column chemistry**

57
58
59
60

1
2
3
4 155 The solutions obtained from previous steps were centrifuged at 5000 rpm for
5
6 156 8 min. Then, as shown in Figure 1, 1 mL of the supernatant solution was passed
7
8
9 157 through a two-layered mixed-resin column (70 mm length \times 6 mm diameter), with the
10
11 158 upper layer containing 1.5 mL of AG50W-X12 (200–400 mesh) resin and bottom
12
13 159 layer containing 0.45 mL of LN Spec resin (100–150 μ m). Before sample loading for
14
15
16 160 separation of Sr-Nd-Hf from the sample matrix, the mixed resin column was
17
18
19 161 pre-washed with 18 mL of 6 M HCl, 8 mL of 3 M HF, and 4 mL of H₂O in turn.

20
21 162 As shown in Table 1 and Figure 2, after sample loading and rinsing four times
22
23 163 with 0.5 mL of 2.5 M HCl, the column was washed with 13.5 mL of 2.5 M HCl. Most
24
25 164 matrix elements (K, Ca, Na, Mg, Al, Fe, Mn, Ti) and Rb were removed during this
26
27
28 165 step. Some Sr (\sim 27 %) was also washed out in this step. Then, the Sr fraction,
29
30
31 166 containing of \sim 71 % Sr, was stripped with 5.5 mL of 2.5 M HCl. Part of the HREEs
32
33 167 (\sim 2 % Dy, \sim 5 % Ho, \sim 14 % Er, \sim 23 % Tm, \sim 11 % Yb, \sim 2 % Lu) and \sim 10 % of
34
35
36 168 Ba were then washed out with 3 mL of 2.5 M HCl. Next, the REEs fraction-enriched
37
38
39 169 Sm+Nd (\geq 96%) was then stripped with 8 mL of 6 M HCl. Sr and the REEs
40
41
42 170 fraction-enriched Sm+Nd were dried on a hotplate at 120 °C to dryness and readied
43
44 171 for TIMS analysis. Residual of Ti on the LN Spec resin was completely washed out
45
46 172 using 15 mL of 3 M HCl + 0.75 % H₂O₂ mixture. Finally, Hf, Zr, Nb, and Ta were
47
48
49 173 extracted from the column with 5 mL of 3.0 M HF. The resulting Hf fraction,
50
51
52 174 containing of \sim 93.4 % Hf, was evaporated on a hotplate at 120°C to dryness, taken up
53
54 175 in 0.05 mL of 0.5 M HF + 0.8 mL 2.0 M HNO₃, and then readied for MC-ICP-MS
55
56 176 analysis. The complete separation procedure, including pre-cleaning of the column,
57
58
59
60

1
2
3
4 177 takes only approximately 9 h for 20 samples or about 70 % less time compared with
5
6 178 conventional three-step column chemistry.
7

8
9 179

10 11 180 **2.4 TIMS for Sr and Nd isotopic analysis** 12

13
14 181 The isotopic compositions of Sr and Nd were measured using a Triton Plus
15
16 182 TIMS instrument (ThermoFisher) at the Institute of Geology and Geophysics, Chinese
17
18 183 Academy of Sciences (IGGCAS) in Beijing, China. Single and double Re filament
19
20
21 184 geometries were used to obtain Sr⁺ and Nd⁺ ion beams, respectively. All Sr and Nd
22
23 185 data were acquired by static multi-collection. The collector array is illustrated in Table
24
25
26 186 2.
27

28
29 187 For Sr isotope ratio measurements, the evaporation filament was heated at 500
30
31 188 mA/min until the ⁸⁸Sr signal reached ~ 20 mV. The beam was centered and roughly
32
33 189 focused, and the evaporation filament was slowly heated to obtain a signal ~ 4 V of
34
35 190 ⁸⁸Sr. Data acquisition was begun when the signal intensity of ⁸⁸Sr had reached ~ 5 V.
36
37
38 191 A peak-center routine was performed prior to data acquisition, and then the baseline
39
40 192 was measured by deflecting the beams using the x-symmetry lens. The measurement
41
42 193 run consisted of 8 ~10 blocks of data with 20 cycles per block. The integration time
43
44 194 per cycle was 4 s. Before mass fractionation correction, the ⁸⁷Sr signal intensity was
45
46 195 corrected for the potential interference caused by the remaining isobaric overlap of
47
48 196 ⁸⁷Rb on ⁸⁷Sr using an ⁸⁷Rb/⁸⁵Rb value of 0.385041.²⁵ After column chemistry, the
49
50 197 ⁸⁵Rb/⁸⁶Sr ratios obtained were $\leq 1 \times 10^{-5}$ in natural silicate sample analysis, showing
51
52
53
54 198 negligible isobaric interference. Finally, the ⁸⁷Sr/⁸⁶Sr ratio data were normalized to
55
56
57
58
59
60

1
2
3
4 199 $^{88}\text{Sr}/^{86}\text{Sr} = 8.375209$ for mass fractionation correction using exponential law. Most of
5
6 200 Sr isotopic data were obtained at an internal precision of $\leq \pm 0.000010$ (2 SE).
7

8
9 201 For Nd isotope ratio measurements, the ionization filament was first heated at a
10
11 202 rate of 450 mA/min to 4.5 A. The evaporation filament was then heated at 400 mA
12
13 203 /min until the ^{146}Nd signal reached 20 mV. Subsequently, the beam was centered and
14
15 204 roughly focused, and the evaporation filament was slowly heated to obtain a ~ 1 V
16
17 205 intensity of ^{146}Nd . Data acquisition was begun once the intensity of ^{146}Nd had reached
18
19 206 ~ 1.2 V. Before the commencement of the analysis, a peak-center routine was run, and
20
21 207 then, the baseline was measured. Data were collected for 8~10 blocks with each block
22
23 208 containing 20 cycles, which, in turn, consisted of 4 s of integration time. The typical
24
25 209 intensity of ^{147}Sm was about ~ 0.4 V during the period of data acquisition. Isobaric
26
27 210 interference from ^{144}Sm can be accurately subtracted following our previously
28
29 211 reported method.²³ After correction of the isobaric interference, the $^{143}\text{Nd}/^{144}\text{Nd}$ ratio
30
31 212 data were normalized to $^{146}\text{Nd}/^{144}\text{Nd} = 0.7219$ for mass fractionation correction using
32
33 213 exponential law. Most of Nd isotopic data were obtained at an internal precision of \leq
34
35 214 ± 0.000010 (2 SE), which was corrected using our off-line program.²³
36
37
38
39
40
41
42
43

44 215 Standards NBS-987 and JNdi-1 were analyzed during the sample measurement
45
46 216 period to monitor instrument status. The NBS-987 standard gave a mean $^{87}\text{Sr}/^{86}\text{Sr}$ of
47
48 217 0.710245 ± 11 (2 SD, $n = 6$), and the JNdi-1 standard gave a mean $^{143}\text{Nd}/^{144}\text{Nd}$ of
49
50 218 0.512109 ± 8 (2 SD, $n = 6$). Both NBS-987 and JNdi-1 standards were good
51
52 219 agreement with previous reported values. All measured $^{87}\text{Sr}/^{86}\text{Sr}$ and $^{143}\text{Nd}/^{144}\text{Nd}$
53
54 220 ratios of silicate samples were normalized to the well-accepted NBS-987 value of
55
56
57
58
59
60

1
2
3
4 221 0.710248¹¹ and JNdi-1 value of 0.512115.²⁶

5
6 222

7
8
9 223 **2.5 MC-ICP-MS for Hf isotopic analysis**

10
11 Hf isotope ratio determinations were carried out using a Thermo Scientific
12
13 Neptune Plus MC-ICP-MS at the IGGCAS in Beijing, China. Detailed descriptions of
14
15 this instrument were previously reported.^{13, 15} Analyses were performed in the static
16
17 mode and cup configurations were shown in Table 2. Typical operating parameters for
18
19 Hf measurement using Neptune Plus were presented in Table 3. A JMC-475 Hf
20
21 standard solution of 100 ppb was used to evaluate the reproducibility and accuracy of
22
23 the instrument during analytical sessions. Each run consisted of a baseline
24
25 measurement and collections of 135~165 cycle that were divided into 9~12 blocks.
26
27
28
29
30
31
32 The integration time of the signals was set to 4 s, and the typical time of one
33
34 measurement lasted for ~ 15 min. A typical sample size used for most samples except
35
36 BIR-1 (30~35 ng) was 100~250 ng. Isobaric interferences of ¹⁷⁶Yb and ¹⁷⁶Lu on ¹⁷⁶Hf
37
38 were monitored by ¹⁷²Yb, ¹⁷³Yb, and ¹⁷⁵Lu. The effects of these interferences were
39
40 corrected on-line using the following values for the stable ratios: ¹⁷⁶Yb/¹⁷³Yb =
41
42 0.79323 and ¹⁷⁶Lu/¹⁷⁵Lu = 0.026528. After one-step column chemistry, Lu/Hf and
43
44 Yb/Hf ratios were generally $\leq 1 \times 10^{-5}$ in natural silicate samples, showing no
45
46
47
48
49 significant difference in ratios before and after interference correction.

50
51 After subtraction of the isobaric interferences, the ¹⁷⁶Hf/¹⁷⁷Hf ratio data were
52
53 directly normalized to ¹⁷⁹Hf/¹⁷⁷Hf = 0.7325 for mass bias correction using exponential
54
55 law.^{13,15} To examine the accuracy of Hf measurement by MC-ICP-MS, samples
56
57
58
59
60

1
2
3
4 243 presented here were interspersed with analyses of the JMC-475 Hf standard. In this
5
6 244 study, 100 ppb of JMC-475 yielded a value of 0.282148 ± 9 (2 SD, $n = 6$), which was
7
8 245 slightly lower than that previously reported. Hence, all measured $^{176}\text{Hf}/^{177}\text{Hf}$ ratios of
9
10 246 silicate samples were normalized to the well-accepted JMC-475 value of 0.282160.¹⁷
11
12
13 247 Last year, 84 analyses of JMC-475 yielded a $^{176}\text{Hf}/^{177}\text{Hf}$ value of 0.282154 ± 18 (2
14
15 248 SD), which was identical to the recommended the well-accepted JMC-475 value of
16
17 249 0.282160,¹⁷ and within the measurement uncertainties.
18
19
20
21
22
23

250

251 3. Results and discussion

252 3.1 Validation of the method and final results

253 To assess the analytical reproducibility and feasibility of our procedure for
254 silicate samples, six CRMs were selected to encompass a wide range of matrix
255 compositions, and analyte concentrations were determined. Because the silicate
256 samples used in the present study had high Sr contents ($\geq 100 \text{ mg.L}^{-1}$), one fifth of the
257 purified Sr fractions and all Nd fractions were loaded on the filament. The sample size
258 of Sr and Nd in TIMS analysis varied significantly, 0.8~3.4 μg for Sr and 0.12~1.6 μg
259 for Nd. For Hf isotope analysis using MC-ICP-MS, the sample consumption was
260 0.03~0.28 μg . Sample sizes were estimated according to the sample weight, recovery
261 of the chemical procedure, and published Sr, Nd, and Hf concentration data.²⁷⁻²⁹

262 During Sr and Nd isotope analyses, as shown in Tables 4 and 5, the $^{87}\text{Sr}/^{86}\text{Sr}$ and
263 $^{143}\text{Nd}/^{144}\text{Nd}$ ratios of all analyzed USGS and GSJ reference materials were obtained
264 with an internal precision better than 0.000013 (2 SE). Average values of $^{87}\text{Sr}/^{86}\text{Sr}$ and

1
2
3
4 265 $^{143}\text{Nd}/^{144}\text{Nd}$ in the present study as well as previous published data are plotted in Figs.
5
6 266 3a and 3b. The $^{87}\text{Sr}/^{86}\text{Sr}$ and $^{143}\text{Nd}/^{144}\text{Nd}$ data presented in the figures agree well with
7
8 267 the previously published data obtained through TIMS or MC-ICP-MS.^{2, 4, 7, 9, 11, 13, 18-20,}
9
10 268 ^{22, 30-32}

11
12
13
14 269 During $^{143}\text{Nd}/^{144}\text{Nd}$ ratio determination, the analyzed objects were REEs instead
15
16 270 of high-purity Nd. Thus, to further examine whether ^{144}Sm can be accurately
17
18 271 subtracted from mixed signals of $^{144}\text{Sm}+^{144}\text{Nd}$ or not, the $^{145}\text{Nd}/^{144}\text{Nd}$ ratio of
19
20 272 silicate samples was also measured and corrected following the previously reported
21
22 273 method.²³ As shown in Table 5 and Figure 4, the corrected $^{145}\text{Nd}/^{144}\text{Nd}$ value is
23
24 274 0.348413 ± 0.000008 (2 SD, $n = 20$) in actual silicate samples, which agrees well with
25
26 275 reported values of $0.348405\sim 0.348419$. The obtained data implied that ^{144}Sm isobaric
27
28 276 interference can be accurately subtracted.^{22, 23, 33-35}

29
30
31
32
33
34 277 For Hf isotope analysis, as shown in Table 6, the $^{176}\text{Hf}/^{177}\text{Hf}$ ratios of most
35
36 278 standard samples except BIR-1 were achieved with an internal precision better than
37
38 279 0.000012 (2 SE). The internal precision ($0.000016\sim 0.000018$, 2 SE) of BIR-1 was
39
40 280 worse than 0.000012 because the Hf concentration of BIR-1 was only 0.6 ppm,²⁷ and
41
42 281 60 mg of BIR-1 materials yielded a small sample size (~ 32 ng) of Hf. The internal
43
44 282 precision of BIR-1 could be improved further by digesting larger amounts of material
45
46 283 (~ 120 mg). Subsequently, the digested sample could be divided into two aliquots.
47
48 284 Each aliquot should be lower than 60 mg and individually separated so that the
49
50 285 purified amalgamated Hf could be obtained sufficient sample sizes (≥ 50 ng). The
51
52 286 average values of $^{176}\text{Hf}/^{177}\text{Hf}$ in this study and previously published data are plotted in
53
54
55
56
57
58
59
60

1
2
3
4 287 Figure 3c. As shown in Figure 3c and Table 6, the $^{176}\text{Hf}/^{177}\text{Hf}$ ratios of all CRMs,
5
6 288 except JA-3 that was slightly lower than the published data, agreed well with
7
8
9 289 previously published data.^{10, 12, 13, 15-17, 36, 37}

10
11 The BCR-2 CRM possesses an excellent homogeneousness and is widely used to
12
13
14 291 monitor the quality of the chemical procedure and the instrumental status in most
15
16 292 geochemical laboratories. Hence, we employ BCR-2 to verify our chemical procedure.
17
18
19 293 The reproducibility of our procedure was demonstrated by ten different dissolutions of
20
21 294 BCR-2 powder materials. As shown in Tables 4, 5, and 6, ten replicate measurements
22
23 295 of BCR-2 yielded a $^{87}\text{Sr}/^{86}\text{Sr}$ value of 0.705010 ± 0.000018 (2 SD), a $^{143}\text{Nd}/^{144}\text{Nd}$
24
25 296 value of 0.512634 ± 0.000010 (2 SD), and a $^{176}\text{Hf}/^{177}\text{Hf}$ value of 0.282885 ± 0.000014
26
27
28 297 (2 SD). The external reproducibility of $^{87}\text{Sr}/^{86}\text{Sr}$, $^{143}\text{Nd}/^{144}\text{Nd}$, and $^{176}\text{Hf}/^{177}\text{Hf}$ ratios of
29
30 298 BCR-2 were better than ± 0.000018 (2 SD), ± 0.000010 (2 SD), and ± 0.000014 (2
31
32 299 SD), respectively.
33
34
35

36 300 In general, the data reproducibility and precision of the proposed method were
37
38 301 satisfactory and completely fitted the demands of geochemistry and petrology.
39
40 302 Practical silicate samples further demonstrated the usefulness and feasibility of our
41
42 303 method.
43
44
45

46 304

49 305 **3.2 Separation protocol**

50
51 306 To avoid isobaric interferences and matrix effects, good chemical separation of
52
53
54 307 Sr-Nd-Hf from the silicate samples is required. Previous studies have revealed that the
55
56 308 AG50W cation resin showed an excellent performance in separating Sr and REEs
57
58
59
60

1
2
3
4 309 from silicate matrix solutions.^{2, 11, 18-20} Similarly, the selectivity of LN spec resin for
5
6 310 Hf allows efficient separation of Hf from silicate matrix solutions.¹³ Further
7
8
9 311 optimization and setup of both LN Spec and AG50W resins are crucial for our
10
11 312 one-step separation procedure. Our proposed procedure features three key points as
12
13
14 313 follows:

15
16 314 First, the order of the resin setup is a crucial consideration. As shown in Figure 1,
17
18 315 1.5 mL and 0.45 mL of AG50W-X12 and LN Spec resins are used as the top and
19
20
21 316 bottom layers, respectively. Reversing the setup order of the AG50W-X12 and LN
22
23 317 Spec resins, Ti and Hf will be re-distributed on the AG50W-X12 resin after removal
24
25
26 318 of the matrix elements and collection of Sr and REEs, resulting in failure of separation
27
28
29 319 between Ti and Hf.

30
31 320 Second, 2.5 M HCl is the most suitable acid to rinse out matrix elements before
32
33 321 collection of Sr, REEs, and Hf. Several HCl concentrations (e.g., 3~4 M) were tested
34
35
36 322 to determine the concentration that best removes the matrix elements. However, the
37
38
39 323 sample purity obtained was unsatisfactory because yellow residues in both the Sr and
40
41
42 324 REE fractions were observed.

43
44 325 Third, the selection of cross-linking degree of AG50W should be carefully
45
46 326 considered. In previous studies, medium cross-linked resin (X8) was preferred
47
48
49 327 because this resin allowed high separation speeds and low experimental costs to
50
51
52 328 purify Sr and REEs. However, for our short column, a more highly cross-linked cation
53
54
55 329 exchange resin (X12, 200–400 mesh) was preferred. The performances of
56
57 330 AG50W-X8 and AG50W-X12 were carefully compared prior to the confirmation of
58
59
60

1
2
3
4 331 the final separation procedure. As the sample loading size increased, the sample purity
5
6 332 of Sr and REEs deteriorated significantly if AG50W-X8 resin was used for separation.
7
8
9 333 In particular, when the loading sample size was larger than 35 mg of silicate material,
10
11 334 e.g., BCR-2, minor matrix elements tailed into the Sr and REE fractions and strongly
12
13
14 335 suppressed the intensities of Sr and Nd signal during TIMS measurement. The sample
15
16 336 loading size would increase to 60 mg and the sample purity of Sr and REEs remained
17
18
19 337 acceptable if a cross-linked (X12) AG50W cation exchange resin was employed.
20
21
22 338

23 339 **3.3 Purity, recovery, and blank**

24
25
26 340 To investigate the behavior of matrix and trace elements retained on the column,
27
28
29 341 a basalt standard material (BCR-2) was employed. A 50 mg of BCR-2 was dissolved
30
31 342 in 1 mL of 2.5 M HCl. Six successive fractions were collected, and corresponding
32
33
34 343 eluting messages were shown in Table 1 and Figure 2. Distribution curves of the
35
36 344 matrix and semi-quantitative trace element analyses were determined using a Thermo
37
38
39 345 Fisher Element-XR ICP-MS instrument.

40
41 346 As shown in Figure 2, most matrix elements (K, Na, Ca, Mg, Al, Fe, Ti), Rb,
42
43
44 347 some Sr (~ 27%), and HREEs were rinsed in fraction 1 before collecting the Sr
45
46 348 fraction. Several residual elements in the Sr fraction (fraction 2), Ba, Er, Tm, and Yb,
47
48
49 349 were found. The yield of Sr in fraction 2 was about 71.0 %. Unwanted elements,
50
51 350 including some HREEs and small amounts of Ti and Sr, were washed out in fraction 3
52
53
54 351 using 3 mL of 2.5 M HCl. Most of the REEs and partly of the Yb (~ 11.4 %) were
55
56 352 stripped in Nd fraction (fraction 4). Most of the Lu (~ 98 %) and Yb (~ 83 %) were
57
58
59
60

1
2
3
4 353 also rinsed out in fraction 4. Generally, few residual elements were observed in the
5
6 354 Nd fraction (fraction 4).
7

8
9 355 Ti must be completely removed from the sample. The use of H₂O₂, which raises
10
11 356 the oxidation state of Ti and forms the yellow-tinted peroxytitanyl compound
12
13 357 Ti(O-O)²⁺ and results in a satisfactory separation of Hf and Ti.³⁸ In the present study,
14
15
16 358 15 mL of 0.075 % H₂O₂ + 3 M HCl was employed to remove Ti. All of the Ti
17
18
19 359 residues were washed out in fraction 5, and most of the Hf +Zr+Ta mixture was rinsed
20
21 360 out in fraction 6. The yield of Hf in fraction 6 was ~ 93.4 %, which was within the
22
23 361 range reported by other investigators.^{9, 10, 13, 38} In summary, the removal efficiency of
24
25
26 362 major elements (Al, Fe, Ca, Mg, K, Na, Ti) was higher than 99.9 % in the Hf fraction
27
28
29 363 (fraction 6).
30

31 364 Procedural blanks are crucial for accurate Sr-Nd-Hf isotope analysis. Blank
32
33 365 values of 170~200, 70~80, and 55~65 pg are obtained for Sr, Nd, and Hf, respectively.
34
35
36 366 For Sr, Nd, and Hf analyses, the blanks are negligible relative to the amount of
37
38
39 367 analytes contained in a 50~60 mg silicate aliquot.
40

41 368

42 369 **4. Conclusions**

43
44
45
46 370 A rapid and robust one-step chemical separation procedure was developed for
47
48 371 measuring ⁸⁷Sr/⁸⁶Sr, ¹⁴³Nd/¹⁴⁴Nd, and ¹⁷⁶Hf/¹⁷⁷Hf isotope ratios in the same sample
49
50
51 372 digest. Sr, Nd, and Hf were sequentially separated from the same rock matrix solution
52
53
54 373 using a single column without intervening evaporation. The chemical separation
55
56 374 scheme was based on the enhanced elemental selectivity permitted by the combined
57
58
59
60

1
2
3
4 375 use of AG50W-X12 cation-exchange and LN Spec resins. This scheme allowed the
5
6 376 use of relatively small columns. The proposed separation procedure achieved the
7
8
9 377 satisfactory and rapid separation of Sr, Nd, and Hf and reduced cross-contamination
10
11 378 risk, thereby offering significant advantages over existing methods in terms of
12
13
14 379 simplicity, separation efficiency, miniaturization, and waste reduction. The potential
15
16 380 fractionation of Sr-Nd-Hf isotopes existed in the chemical resin column could be
17
18
19 381 corrected by using the traditional internal correction methods. The bottleneck
20
21 382 associated with sample preparation prior to thermal ionization mass spectrometric
22
23
24 383 measurements can be significantly reduced with the new protocol. An alternative
25
26 384 approach to the measurement of these isotope ratios using MC-ICP-MS could be
27
28
29 385 considered. In the present investigation this would involve modifications of the
30
31 386 column protocols, especially in the case of Sr.

32
33
34 387

35 36 388 **Acknowledgements**

37
38
39 389 This work was jointly supported by the National Natural Science Foundation of
40
41 390 China (grants 41273021 and 41373020) and the State Key Laboratory of Lithospheric
42
43
44 391 Evolution (grant 11301520), Institute of Geology and Geophysics, Chinese Academy
45
46 392 of Sciences.

47
48
49 393

50
51 394

52
53
54 395

55
56 396
57
58
59
60

397

398 **References:**

- 399 1. J.P. Davidson, D.J. Morgan, B.L.A. Charlier, R. Harlou, J.M. Hora, *Annu. Rev.*
400 *Earth Planet Sci.*, 2007, 35, 273-311.
- 401 2. C. Na, T. Nakano, K. Tazawa, M. Sakagawa, T. Ito, *Chem. Geol.*, (Isotope
402 *Geoscience Section*), 1995, 123, 225-237.
- 403 3. C. Pin, D. Briot, C. Bassin, E. Poitrasson, *Anal. Chim. Acta.*, 1994, 298, 209-217.
- 404 4. C. Pin, J. Francisco, S. Zalduegui, *Anal. Chim. Acta.*, 1997, 339, 79-89.
- 405 5. Y. Arakawa, *Geochem. J.*, 1992, 26, 105-109.
- 406 6. C. F. Li, F. K. Chen and X. H. Li, *Int. J. Mass Spectrom.*, 2007, 266, 34-41.
- 407 7. Z. Y. Chu, F. K. Chen, Y. H. Yang, J. H. Guo, *J. Anal. At. Spectrom.*, 2009, 24,
408 1534-1544.
- 409 8. X.J. Yang, C. Pin, *Anal. Chem.*, 1999, 71, 1706-1711.
- 410 9. B. Lefvre, C. Pin, *Anal. Chim. Acta.*, 2005, 543, 209-221.
- 411 10. J.N. Connelly, D.G. Ulfbeck, K. Thrane, M. Bizzarro, T. Housh, *Chem. Geol.*,
412 2006, 233, 126-136.
- 413 11. D. Weis, B. Kieffer, C. Maerschalk, J. Barling, J. D. Jong, G. A. Williams, D.
414 Hanano, W. Pretorius, N. Mattielli, J. S. Scoates, A. Goolaerts, R. M. Friedman
415 and J. B. Mahoney, *Geochem. Geophys. Geosyst.*, 2006, DOI:
416 10.1029/2006GC001283.
- 417 12. B. Lefvre, C. Pin, *Anal. Chem.*, 2001, 73, 2453-2460.
- 418 13. Y.H. Yang, H.F. Zhang, Z.Y. Chu, L.W. Xie, F.Y. Wu, *Int. J. Mass Spectrom.*,

- 1
2
3
4 419 2010, 290, 120-126.
5
6 420 14. A. Makishima, E. Nakamura, *Geochem. J.*, 2008, 42, 199-206.
7
8 421 15. Y.H. Yang, F.Y. Wu, S.A. Wilde, L.W. Xie, *Int. J. Mass Spectrom.*, 2011, 299,
9
10 422 47-52.
11
12 423 16. N.C. Chu, R.N. Taylor, V. Chavagnac, R.W. Nesbitt, R.M. Boella, J.A. Milton,
13
14 424 C.R. German, G. Bayon, K. Burton, *J. Anal. At. Spectrom.*, 2002, 17, 1567-1574.
15
16 425 17. M. Bizzarro, J.A. Baker, D. Ulfbeck, *Geostand. Newslett.*, 2003, 27, 133-145.
17
18 426 18. Y. Orihashi, J. Maeda, R. Tanaka, R. Zeniya, K. Niida, *Geochem. J.*, 1998, 32,
19
20 427 205-211.
21
22 428 19. T. Miyazaki, K. Shuto, *Geochem. J.*, 1998, 32, 345-350
23
24 429 20. C.F. Li, X.H. Li, Q.L. Li, J.H. Guo, X.H. Li, T. Liu, *Anal. Chim. Acta.*, 2011,
25
26 430 706, 297-305.
27
28 431 21. M. Griselin, J.C.V. Belle, C. Pomies, P.Z. Vroon, M.C.V. Soest, G.R. Davies,
29
30 432 *Chem. Geol.*, 2001, 172, 347-359.
31
32 433 22. Y.H. Yang, F.Y. Wu, L.W. Xie, Y.B. Zhang, *Anal. Lett.*, 2010, 43, 142-150.
33
34 434 23. C.F. Li, X.H. Li, Q.L. Li, J.H. Guo, X.H. Li, *J. Anal. At. Spectrom.*, 2011, 26,
35
36 435 2012-2022.
37
38 436 24. I.C. Kleinmanns, K. Kreissig, B.S. Kamber, T. Meisel, T.F. Nagler, J.D. Kramers,
39
40 437 *Anal. Chem.*, 2002, 74, 67-73.
41
42 438 25. B.L.A. Charlier, C. Ginibre, D. Morgan, G.M. Nowell, D.G. Pearson, J.P.
43
44 439 Davidson, C.J. Ottley, *Chem. Geol.*, 2006, 232, 114-133.
45
46 440 26. T. Tanaka, S. Togashi, H. Kamioka, H. Amakawa, H. Kagami, T. Hamamoto, M.
47
48
49
50
51
52
53
54
55
56
57
58
59
60

- 1
2
3
4 441 Yuhara, Y. Orihashi, S. Yoneda, H. Shimizu, T. Kunimaru, K. Takahashi, T.
5
6 442 Yanagi, T. Nakano, H. Fujimaki, R. Shinjo, Y. Asahara, M. Tanimizu and C.
7
8
9 443 Dragusanu, *Chem. Geol.*, 2000, 168, 279-281.
10
11 444 27. P. Dulski, *Geostand. Newslett.*, 2001, 25, 87-125.
12
13 445 28. M. Willbold, K.P. Jochum, *Chem. Geol.*, 2005, 29, 63-82.
14
15
16 446 29. R. L. Korotev, *Geostand. Newslett.*, 1996, 20, 217-245.
17
18
19 447 30. C.F. Li, X.H. Li, Q.L. Li, J.H. Guo, X.H. Li, L.J. Feng, Z.Y. Chu, *Anal.*
20
21 448 *Chem.*, 2012, 84, 6040-6047.
22
23 449 31. C.F. Li, X.H. Li, Q.L. Li, J.H. Guo, X.H. Li, Y.H. Yang, *Anal. Chim. Acta.*,
24
25 450 2012, 727, 54-60.
26
27
28 451 32. Y.H. Yang, F.Y. Wu, Z.C. Liu, Z.Y. Chu, L.W. Xie, J.H. Yang, *J. Anal. At.*
29
30 452 *Spectrom.*, 2012, 27, 516-522.
31
32
33 453 33. B. Luais, P. Telouk and F. Albarede, *Geochim. Cosmochim. Acta.*, 1997, 61,
34
35 454 4847-4854.
36
37
38 455 34. G. Caro, B. Bourdon, J.L. Birck, S. Moorbath, *Geochim. Cosmochim. Acta.*, 2006,
39
40 456 70, 164-191.
41
42
43 457 35. G. J. Wasserburg, S. B. Jacobsen, D. J. DePaolo, M. T. McCulloch and T. Wen,
44
45 458 *Geochim. Cosmochim. Acta.*, 1981, 45, 2311-2323.
46
47
48 459 36. T. Hanyu, S. Nakai, R. Tatsuta, *Geochem. J.*, 2005, 39, 83-90.
49
50
51 460 37. Y.H. Lu, A. Makishima, E. Nakamura, *J. Anal. At. Spectrom.*, 2007, 22, 69-76.
52
53
54 461 38. C. Munker, S. Weyer, E. Scherer, K. Mezger, *Geochem. Geophys. Geosyst.*, 2001,
55
56 462 DOI: 2.10.1029/2001GC000183.
57
58
59
60

1
2
3
4 463

5
6 **Figure captions**
7

8
9 465 **Fig 1.** Single-step separation scheme in this study compared with the traditional
10
11 466 three-step separation procedure.

12
13 467 **Fig 2.** Distribution curve of all eluted fractions of BCR-2 in the mixed AG50W-12 +
14
15
16 468 LN Spec resin column.

17
18
19 469 **Fig 3.** Comparison of Sr-Nd-Hf values obtained by the present study and previous
20
21 470 data.

22
23
24 471 **Fig 4.** Corrected $^{145}\text{Nd}/^{144}\text{Nd}$ ratios for silicate rock from USGS and GSJ.
25
26
27
28
29
30
31
32
33
34
35
36
37
38
39
40
41
42
43
44
45
46
47
48
49
50
51
52
53
54
55
56
57
58
59
60

Table 1. Single-step chemical procedure for Sr-Nd-Hf separation

Procedure	Eluting reagent		Eluting volume (mL)	Eluting Fraction
Loading sample	2.5M	HCl	1.0	1
Rinsing	2.5M	HCl	2.0 (0.5 x 4)	1
Rinsing	2.5M	HCl	13.5	1
Eluting Sr	2.5M	HCl	5.5	2
Rinsing	2.5M	HCl	3.0	3
Eluting Nd	6.0M	HCl	8.0	4
Rinsing	3.0M HCl + 0.75 % H ₂ O ₂		15.0	5
Eluting Hf	3.0M	HF	5.0	6

Table 2. Cup configuration for Sr-Nd isotope analysis using Triton plus TIMS and for Hf isotope analysis using Neptune plus MC-ICP-MS

Element	L4	L3	L2	L1	CC	H1	H2	H3	H4
Sr			⁸⁴ Sr	⁸⁵ Rb	⁸⁶ Sr	⁸⁷ Sr	⁸⁸ Sr		
Nd	¹⁴³ Nd	¹⁴⁴ Nd+ ¹⁴⁴ Sm	¹⁴⁵ Nd	¹⁴⁶ Nd	¹⁴⁷ Sm	¹⁴⁹ Sm			
Hf	¹⁷² Yb	¹⁷³ Yb	¹⁷⁵ Lu	¹⁷⁶ Hf	¹⁷⁷ Hf	¹⁷⁸ Hf	¹⁷⁹ Hf	¹⁸⁰ Hf	¹⁸² W

Table 3. Typical operating parameters for Hf measurement using**Neptune Plus MC-ICP-MS**

Neptune Plus MC-ICP-MS	Setting
RF forward power	1300 W
Cooling gas	15.5 L/min
Auxiliary gas	0.7 L/min
Aerosol carrier gas	~ 1.10 L/min (optimized daily)
Extraction	- 2000 V
Focus	- 645 V
Detection system	Nine Faraday collectors
Acceleration voltage	10 kV
Interface cones	Nickel
Spray chamber	Glass cyclonic
Nebulizer type	Micromist PFA nebulizer
Sample uptake rate	50 μ L/min
Uptake mode	Free aspiration
Instrument Resolution	~ 400 (Low)
Typical sensitivity on ^{180}Hf	~ 16 V/ppm (10^{11} Ω resistors)
Sampling mode	9~12 blocks of 15 cycles
Integration time	4 sec
Analytical time	~ 660 sec
Baseline	ca. 1 min on peak in 2% HNO_3

Table 4. Analytical results of $^{87}\text{Sr}/^{86}\text{Sr}$ ratios for CRMs determined by Triton Plus TIMS

CRMs	Raw $^{87}\text{Sr}/^{86}\text{Sr}$	Corrected $^{87}\text{Sr}/^{86}\text{Sr}$	2 SE	Reported value	Rb/Sr ratio
BCR-2	0.702128	0.705018	0.000012	0.705019 ¹¹ ; 0.705023 ¹³	0.1395 ²⁸
BCR-2	0.705617	0.705002	0.000012	0.705026 ³¹ ; 0.704998 ³²	
BCR-2	0.708509	0.705004	0.000012		
BCR-2	0.702479	0.705005	0.000009		
BCR-2	0.708523	0.704999	0.000010		
BCR-2	0.703277	0.705018	0.000011		
BCR-2	0.705146	0.705023	0.000010		
BCR-2	0.701334	0.705015	0.000011		
BCR-2	0.702338	0.705002	0.000009		
BCR-2	0.701511	0.705021	0.000010		
Mean \pm 2 SD		0.705010	0.000018	0.705017	
W-2	0.707856	0.706983	0.000009	0.706966 ¹³ ; 0.706973 ³¹	0.1010 ²⁷
W-2	0.712276	0.706997	0.000010		
Mean		0.706990		0.706970	
BHVO-2	0.704378	0.703470	0.000011	0.703487 ¹¹ ; 0.703479 ³¹	0.0217 ²⁸
BHVO-2	0.711143	0.703488	0.000010	0.703468 ³² ;	
Mean		0.703479		0.703478	
JA-1	0.703465	0.703543	0.000008	0.703533 ² ; 0.703557 ¹⁸	0.044 ²⁹

1
2
3
4
5
6
7
8
9
10
11
12
13
14
15
16
17
18
19
20
21
22
23
24
25
26
27
28
29
30
31
32
33
34
35
36
37
38
39
40
41
42
43
44
45
46
47
48
49

JA-1	0.706042	0.703529	0.000009	0.703543 ¹⁹	
Mean		0.703536		0.703544	
JA-3	0.705905	0.704172	0.000010	0.704160 ¹⁹ ; 0.704177 ³¹	0.1232 ²⁷
JA-3	0.707787	0.704169	0.000008		
Mean		0.704171		0.704169	
BIR-1	0.705128	0.703117	0.000010	0.703130 ³¹ ; 0.703108 ³²	0.0033 ²⁷
BIR-1	0.704220	0.703114	0.000011		
Mean		0.703116		0.703119	
NBS-987	0.706769	0.710246	0.000011		
	0.706296	0.710254	0.000010		
	0.708337	0.710244	0.000009		
	0.706772	0.710249	0.000009		
	0.705853	0.710241	0.000010		
	0.707506	0.710238	0.000010		
Mean ± 2 SD		0.710245	0.000011		

Table 5. Analytical results of $^{143}\text{Nd}/^{144}\text{Nd}$ ratios for CRMs determined using TIMS without Nd and Sm separation

CRMs			Reported Values				
	Raw $^{143}\text{Nd}/^{144}(\text{Nd}+\text{Sm})$	Corrected $^{143}\text{Nd}/^{144}\text{Nd}$	2 SE	$^{145}\text{Nd}/^{144}\text{Nd}$	2 SE	$^{143}\text{Nd}/^{144}\text{Nd}$	Sm/Nd
BCR-2	0.497824	0.512631	0.000008	0.348413	0.000006	0.512632^6 ; 0.512641^7	0.224^{28}
BCR-2	0.501391	0.512640	0.000006	0.348412	0.000004	0.512634^{11} ; 0.512640^{13}	
BCR-2	0.504291	0.512636	0.000006	0.348414	0.000004	0.512630^{20} ; 0.512638^{22}	
BCR-2	0.500965	0.512629	0.000005	0.348414	0.000003	0.512630^{23} ; 0.512638^{30}	
BCR-2	0.471586	0.512642	0.000008	0.348414	0.000005	0.512636^{31}	
BCR-2	0.510027	0.512635	0.000005	0.348411	0.000003		
BCR-2	0.495168	0.512633	0.000005	0.348411	0.000003		
BCR-2	0.491770	0.512630	0.000004	0.348411	0.000002		
BCR-2	0.502585	0.512635	0.000005	0.348411	0.000002		
BCR-2	0.501244	0.512627	0.000008	0.348414	0.000004		
Mean \pm 2 SD		0.512634	0.000010	0.348413	0.000003	0.512635	
W-2	0.478999	0.512525	0.000010	0.348416	0.000008	0.512510^4 ; 0.512537^7 ; 0.512516^{13}	0.254^{27}
W-2	0.488623	0.512521	0.000012	0.348415	0.000008	0.512511^{22} ; 0.512528^{30}	
Mean		0.512523		0.348416		0.512520	
BHVO-2	0.463961	0.512971	0.000006	0.348409	0.000005	0.512989^6 ; 0.512951^7 ; 0.512981^{11}	0.247^{28}
BHVO-2	0.494408	0.512981	0.000008	0.348409	0.000005	0.512984^{22} ; 0.512985^{23} ; 0.512983^{30}	
Mean		0.512976		0.348409		0.512979	

1								
2								
3								
4								
5								
6								
7	JA-1	0.489061	0.513080	0.000012	0.348406	0.000009	0.513066 ² ; 0.513107 ⁹	0.343 ²⁹
8	JA-1	0.490259	0.513094	0.000010	0.348406	0.000009	0.513078 ¹⁸ ; 0.513092 ¹⁹	
9	Mean		0.513087		0.348406		0.513086	
10								
11								
12	JA-3	0.487184	0.512841	0.000012	0.348413	0.000008	0.512835 ⁶ ; 0.512859 ¹⁹	0.248 ²⁷
13	JA-3	0.495082	0.512851	0.000012	0.348414	0.000010	0.512840 ²³ ; 0.512859 ³⁰	
14	Mean		0.512846		0.348414		0.512848	
15								
16								
17								
18								
19	BIR-1	0.425078	0.513106	0.000012	0.348425	0.000008	0.513107 ⁷ ; 0.513108 ⁹	0.460 ²⁷
20	BIR-1	0.463980	0.513095	0.000014	0.348417	0.000010	0.513093 ²⁰ ; 0.513084 ²³	
21	Mean		0.513101		0.348421		0.513098	
22								
23								
24	JNdi-1	0.512576	0.512110	0.000008				
25		0.512662	0.512117	0.000007				
26		0.511807	0.512107	0.000008				
27		0.511720	0.512106	0.000008				
28		0.512935	0.512109	0.000009				
29		0.512539	0.512107	0.000007				
30	Mean ± 2 SD		0.512109	0.000008				
31								
32								
33								
34								
35								
36								
37								
38								
39								
40								
41								
42								
43								
44								
45								
46								
47								
48								
49								

Table 6. Analytical results of $^{176}\text{Hf}/^{177}\text{Hf}$ ratios for CRMs determined by Neptune Plus MC-ICP-MS

CRMs	Raw $^{176}\text{Hf}/^{177}\text{Hf}$	Corrected $^{176}\text{Hf}/^{177}\text{Hf}$	2 SE	Reported Value	Lu/Hf	Yb/Hf
BCR-2	0.279622	0.282883	0.000006	0.282869 ¹⁰ ; 0.282884 ¹² ; 0.282877 ¹³	0.106 ²⁸	0.709 ²⁸
BCR-2	0.279592	0.282877	0.000006	0.282859 ¹⁶ ; 0.282875 ¹⁷ ; 0.282895 ³⁶		
BCR-2	0.279581	0.282879	0.000006			
BCR-2	0.279608	0.282895	0.000006			
BCR-2	0.279576	0.282880	0.000008			
BCR-2	0.279608	0.282884	0.000010			
BCR-2	0.279606	0.282895	0.000006			
BCR-2	0.279621	0.282888	0.000010			
BCR-2	0.279623	0.282877	0.000010			
BCR-2	0.279599	0.282888	0.000012			
Mean \pm 2 SD		0.282885	0.000014	0.282875		
W-2	0.279652	0.282742	0.000008	0.282715 ¹² ; 0.282724 ¹³	0.133 ²⁷	0.871 ²⁷
W-2	0.279623	0.282723	0.000008	0.282715 ¹⁵		
Mean		0.282733		0.282718		
BHVO-2	0.279880	0.283101	0.000012	0.283094 ¹⁵ ; 0.283116 ¹⁷	0.061 ²⁸	0.454 ²⁸
BHVO-2	0.279874	0.283097	0.000013			
Mean		0.283099		0.283105		
JA-1	0.279941	0.283269	0.000012	0.283250 ⁹ ; 0.283258 ¹²	0.169 ²⁹	1.14 ²⁹
JA-1	0.279911	0.283247	0.000013	0.283292 ³⁶ ; 0.283264 ³⁷		

1
2
3
4
5
6
7
8
9
10
11
12
13
14
15
16
17
18
19
20
21
22
23
24
25
26
27
28
29
30
31
32
33
34
35
36
37
38
39
40
41
42
43
44
45
46
47
48
49

Mean		0.283258		0.283266		
JA-3	0.279773	0.283046	0.000010	0.283084 ³⁶ ; 0.283063 ³⁷	0.461 ²⁷	0.566 ²⁷
JA-3	0.279778	0.283057	0.000008			
Mean		0.283052		0.283074		
BIR-1	0.280145	0.283292	0.000016	0.283247 ⁹ ; 0.283291 ¹²	0.417 ²⁷	2.73 ²⁷
BIR-1	0.280138	0.283283	0.000018	0.283277 ¹⁷ ; 0.283265 ³⁶		
Mean		0.283288		0.283270		
JMC-475	0.278803	0.282154	0.000008			
	0.278901	0.282151	0.000008			
	0.278815	0.282145	0.000008			
	0.278804	0.282143	0.000007			
	0.278808	0.282144	0.000006			
	0.278874	0.282148	0.000006			
Mean ± 2 SD		0.282148	0.000009			

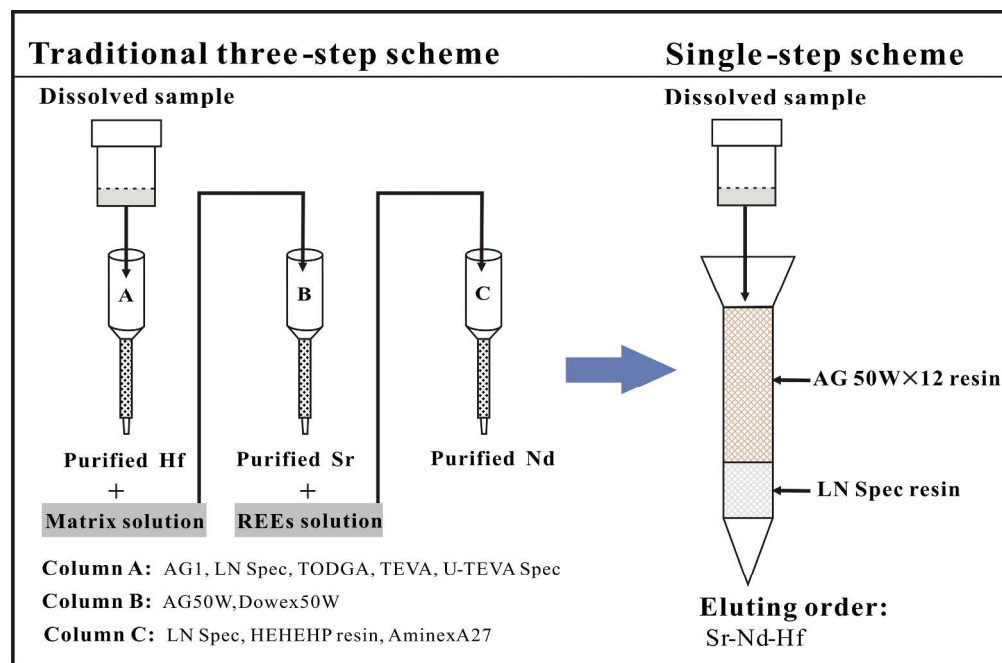


Figure 1
131x86mm (600 x 600 DPI)

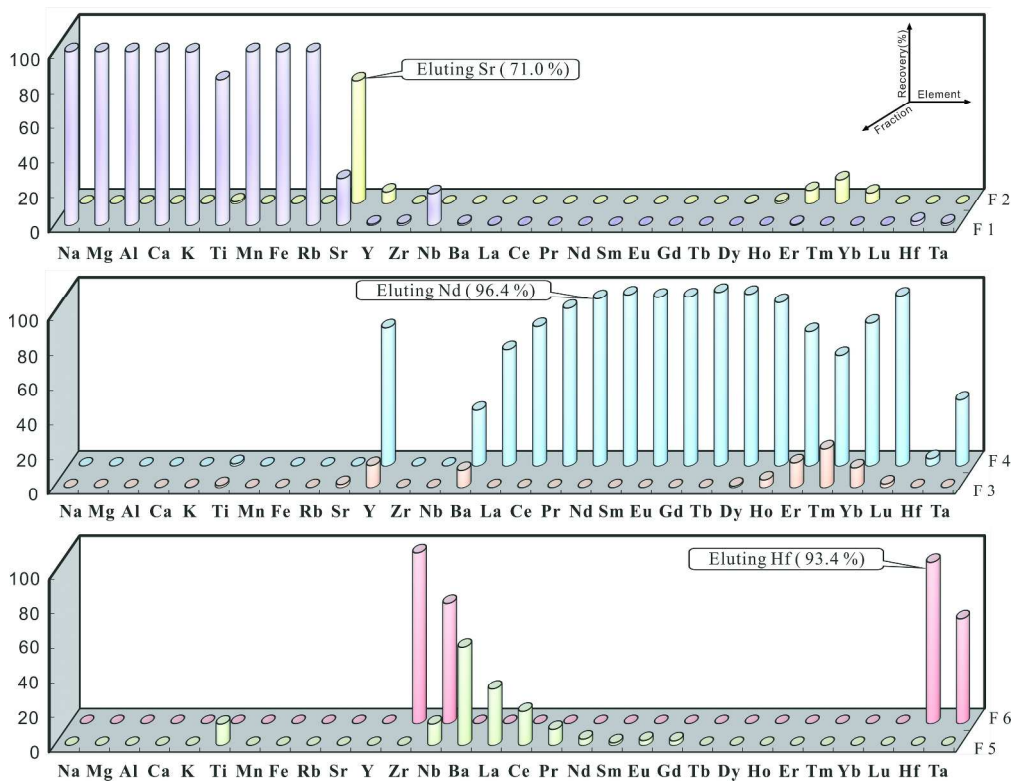


Figure 2
154x119mm (600 x 600 DPI)

1
2
3
4
5
6
7
8
9
10
11
12
13
14
15
16
17
18
19
20
21
22
23
24
25
26
27
28
29
30
31
32
33
34
35
36
37
38
39
40
41
42
43
44
45
46
47
48
49
50
51
52
53
54
55
56
57
58
59
60

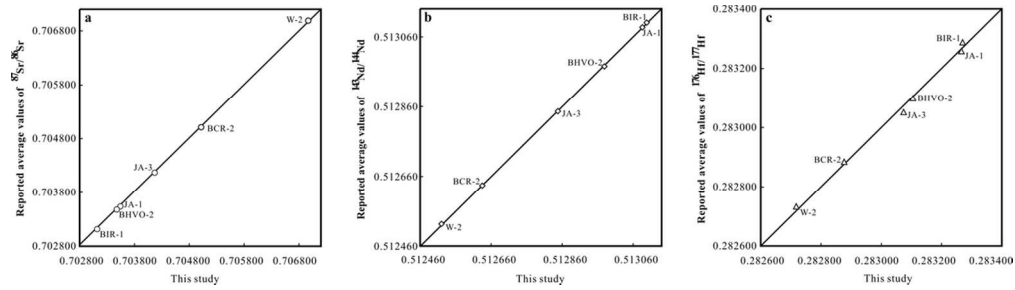


Figure 3
55x15mm (600 x 600 DPI)

1
2
3
4
5
6
7
8
9
10
11
12
13
14
15
16
17
18
19
20
21
22
23
24
25
26
27
28
29
30
31
32
33
34
35
36
37
38
39
40
41
42
43
44
45
46
47
48
49
50
51
52
53
54
55
56
57
58
59
60

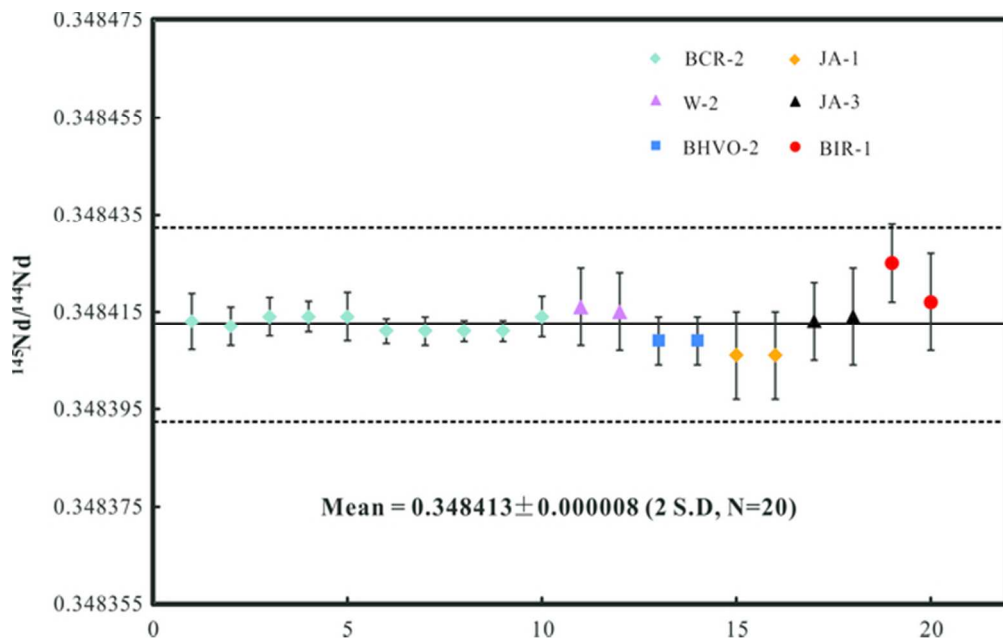


Figure 4
56x35mm (300 x 300 DPI)